

- supporting this phylogenetic hypothesis (5, 6).
9. For detailed stratigraphic information, see W. E. Stein, Jr., D. C. Wight, and C. B. Beck, *Can. J. Bot.* **61**, 1283 (1983).
  10. K. Esau, *The Phloem* (Borntraeger, Berlin, 1969).
  11. Techniques used in preparing this specimen are detailed in W. E. Stein, D. C. Wight, and C. B. Beck, *Rev. Palaeobot. Palynol.* **36**, 185 (1982).
  12. J. Galtier and C. Hébert, *C. R. Acad. Sci. Ser. D* **267**, 2257 (1973).
  13. J. W. Hall, *Am. Midl. Nat.* **47**, 763 (1952); G. W. Rothwell, *Palaeontogr. Abt. B Palaeophytol.* **151**, 171 (1975).
  14. T. Delevoryas and J. Morgan, *ibid.* **96**, 12 (1954); W. N. Stewart, *Am. J. Bot.* **38**, 709 (1951); W. C. Williamson and D. H. Scott, *Philos. Trans. R. Soc. London Ser. B* **186**, 703 (1895).
  15. W. N. Stewart, *Trans. Ill. State Acad. Sci.* **33**, 54 (1940); *Am. J. Bot.* **34**, 315 (1947); E. L.

- Smoot and T. N. Taylor, *Science* **202**, 1081 (1978); E. L. Smoot, *Am. J. Bot.* **66**, 511 (1979); K. B. Pigg and G. W. Rothwell, *Bot. Gaz. (Chicago)* **144**, 132 (1983).
16. D. F. Satterthwait and J. W. Schopf [*Am. J. Bot.* **59**, 373 (1972)] describe cells that they consider to be conducting elements of the phloem in *Rhynia major*, a fossil plant from the Lower Devonian of Scotland. However, their data, although suggestive, are, we believe, insufficient for a positive determination.
17. K. Esau, V. I. Cheadle, E. F. Gifford, *Am. J. Bot.* **40**, 9 (1953).
18. C. G. K. Ramanujam and W. N. Stewart, *ibid.* **56**, 101 (1969).
19. Supported by NSF grant BSR-8113542 to C. B. B. We thank W. H. Wagner, T. Johns, and M. A. Cichan for helpful suggestions concerning the manuscript.

16 May 1984; accepted 18 July 1984

## Rayleigh-Benard Convection in an Electrochemical Redox Cell

**Abstract.** *Damped voltage oscillations occur when current steps are applied to a cell consisting of a thin layer of  $\text{Fe}^{111}/\text{Fe}^{11}$  electrolyte sandwiched between horizontal, parallel, platinized platinum electrodes. The upper electrode must be the anode, and the magnitude of the current must be larger than a threshold value. The oscillations signal the onset of convection in the fluid. The experiment provides a new method for investigating transient convection processes.*

We report here what we believe are previously unobserved phenomena in a simple, well-studied electrochemical system, the ferrous-ferric redox cell. We used horizontal, platinized platinum electrodes,  $5.1 \text{ cm}^2$  in area, spaced a distance,  $d$ ,  $0.94$  to  $3 \text{ mm}$  apart (1). The electrolyte was  $0.05M \text{ FeCl}_2$ ,  $0.05M \text{ FeCl}_3$ , and  $1M \text{ HCl}$  in water (2). Steps of constant current,  $i$ , were applied, and the voltage,  $V(t)$ , was measured as a function of time.

When the top electrode was negative or when it was positive and  $i$  was small,  $V(t)$  exhibited the monotonic transients that one expects (3) for diffusion-controlled kinetics (the dashed curve in Fig. 1). Interesting effects (the solid curve in Fig. 1) occurred only when the top electrode was positive and  $i$  was larger than a threshold value,  $i_c$ . Then  $V(t)$  followed the diffusion transient at first but suddenly fell away, executed a series of damped oscillations, and came to a steady value less than that with the cathode up. When  $i$  was turned off,  $V(t)$  rapidly reversed sign and then decayed slowly.

The oscillation period increased with decreasing  $i$  and became infinitely long as  $i$  approached  $i_c$ , which made it difficult to determine  $i_c$  precisely by observing whether oscillations occurred or not with a given  $i$  (a graphical method is described later). The oscillations decayed with a time constant close to the rise time of the cathode-up curve, independent of  $i$  and proportional to  $d^2$ . In a few experiments the potentials of the platinum electrodes were measured with respect to a  $\text{Ag}/\text{AgCl}$  electrode. They were opposite

in sign and equal in magnitude (to  $\approx 0.5 \text{ mV}$ ) at all times, even during the oscillations.

Convection in the fluid was observed when  $0.79\text{-}\mu\text{m}$  latex polystyrene spheres were added and they were viewed with scattered light, with the observer looking through a telescope in a direction parallel to the electrodes (4). The spheres moved continuously when the anode was up and  $i > i_c$ , otherwise not at all. Those moving in planes normal to the line of sight, thus staying in focus, were seen to execute square-shaped, closed orbits. Their orbital periods were close to the period of the voltage oscillation that had occurred when  $i$  was first applied. When  $i$  was turned off, the particles executed half an orbit more and then came to rest.

These phenomena manifest Rayleigh-Benard convection (5–7), a process that occurs in nature when a fluid is heated from below. It customarily is induced in laboratory experiments in the same way. The following arguments suggest that in our experiment, as in those of a few

earlier investigators (8, 9), the density gradients that drive convection result from composition gradients rather than temperature gradients in the fluid.

In either case, a density difference,  $\Delta\rho$ , is created between the top and bottom of the fluid. If  $\Delta\rho$  exceeds a critical threshold value, convection occurs. Theory shows that the threshold is determined solely by the value of the Rayleigh number

$$Ra = g\Delta\rho d^3/\mu D \quad (1)$$

Here  $g$  is the acceleration of gravity,  $\mu$  is the viscosity, and  $D$  is the diffusion constant with which density gradients are dissipated by diffusion processes in the fluid (for example, for thermally induced convection  $D$  is the thermal diffusivity). Convection begins when  $Ra$  exceeds a critical value,  $Ra_c$ , calculable at the outset; for our boundary conditions,  $Ra_c = 1707.76$ . Testing our observations against this prediction, we conclude that convection in our experiments cannot be thermally driven. All thermoelectric effects that are possible (10) would produce small values of  $\Delta\rho$  and  $Ra \ll Ra_c$ .

To perform the same test assuming that convection is composition-driven, we must first deduce values of  $\Delta\rho$  and  $D$  to be inserted in Eq. 1 in that case. Several features of the electrochemistry simplify this analysis. Reactions at the platinized electrodes are fast. Overall kinetics are limited by transport of  $\text{Fe}^{11}$  and  $\text{Fe}^{111}$ . Because the electric field in the electrolyte is negligible (11), the transport of these ions occurs by diffusion (if there is no convection) or by diffusion plus convection. We determined (12) the diffusion constants of  $\text{Fe}^{11}$  and  $\text{Fe}^{111}$  and found them to be the same within experimental error,  $D = (6.2 \pm 0.5) \times 10^{-10} \text{ m}^2/\text{sec}$  at  $25^\circ\text{C}$  (13). The equality of the diffusion constants means that double-diffusion effects (7) do not appear.

It also simplifies the way in which electrolysis affects composition and hence  $\Delta\rho$ . A fraction of the  $\text{FeCl}_2$  immediately adjacent to the anode is replaced

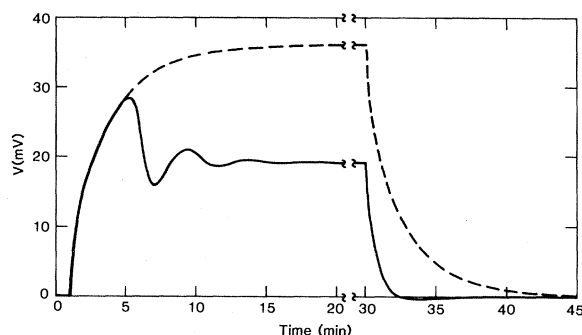


Fig. 1. Voltage plotted as a function of time. A current of  $1 \text{ mA}$  was applied at  $1 \text{ minute}$  and removed at  $30 \text{ minutes}$ ;  $d = 1 \text{ mm}$ . The dashed curve was obtained with the cathode up, the solid curve with the anode up.

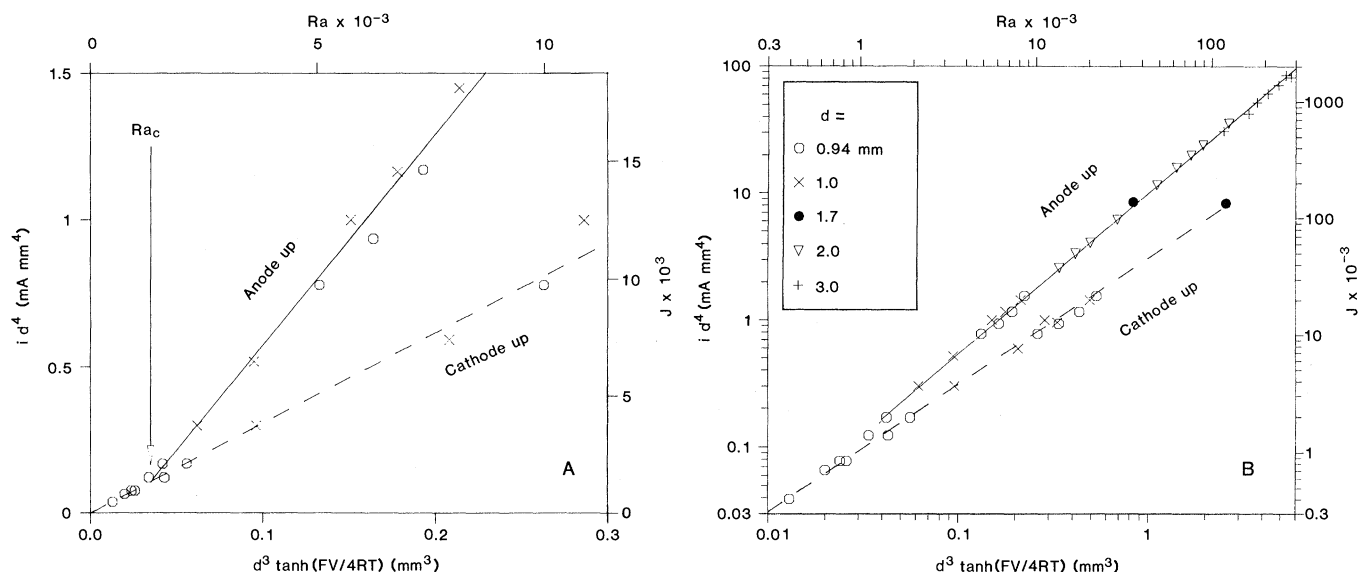


Fig. 2. Steady-state  $i$ - $V$  data plotted in the form suggested by theory. Values of  $Ra$  and  $J$  are computed from the observables  $i$ ,  $d$ , and  $V$  as described in the text. (A) Linear plot of data for low  $Ra$ . The threshold for convection is at the intersection of the lines. (B) A log-log plot of all data. The anode-up data fit to  $J = k Ra^n$  with  $k = 0.286 \pm 0.001$ ,  $n = 1.272 \pm 0.006$ , in good agreement with analogous thermal convection results (15).

by  $\text{FeCl}_3$ , an equal fraction of the  $\text{FeCl}_3$  at the cathode is replaced by  $\text{FeCl}_2$ , and  $\text{HCl}$  is everywhere unaffected (approximately). The maximum possible composition (and density) difference is realized when  $[\text{Fe}^{II}] = 0$  at the anode and  $[\text{Fe}^{III}] = 0$  at the cathode, that is, when there is  $0.1M$   $\text{FeCl}_3$  and  $1M$   $\text{HCl}$  at the anode, and  $0.1M$   $\text{FeCl}_2$  and  $1M$   $\text{HCl}$  at the cathode. We measured the specific gravities of these two solutions and found them to differ by  $22 \pm 2 \times 10^{-4}$  at  $25^\circ\text{C}$ . The  $\text{FeCl}_3$ -rich solution is the denser, consistent with the observed convection effects.

That datum is combined with  $V(t)$  in the following way to estimate  $\Delta\rho$ . Let  $c_o$  represent the mean concentration of  $\text{Fe}^{II}$  and  $\text{Fe}^{III}$  ( $0.05M$ ). Let  $\Delta c(t)$  represent the instantaneous increase in  $[\text{Fe}^{III}]$  and decrease in  $[\text{Fe}^{II}]$  at the anode caused by electrolysis, and also the equal and opposite changes at the cathode. The cell voltage is given by the Nernst potential,

$$(RT/F) \ln([\text{Fe}^{III}]/[\text{Fe}^{II}])$$

at the anode less than at the cathode, where  $R$  is the gas constant,  $T$  is the absolute temperature, and  $F$  is the faraday. Expressing the concentrations at the electrodes in terms of  $c_o \pm \Delta c(t)$  and solving for  $\Delta c(t)$  yields

$$\Delta c(t) = c_o \tanh[FV(t)/4RT] \quad (2)$$

Finally,  $\Delta\rho$  is estimated as

$$\Delta\rho = (d\rho/dc) \times \Delta c(t) \quad (3)$$

where  $d\rho/dc = 44 \times 10^{-3} \text{ kg/mol}$  (as determined by the specific gravity measurements).

Steady-state  $Ra$  values calculated

from the data in this manner are shown in Fig. 2. The form of these plots was chosen by dimensional analysis so the data for all  $d$  would fall on two curves, one for cathode up (no convection) and one for anode up (with convection). The abscissa is proportional to  $Ra$ , the ordinate to the dimensionless current density,  $J = id^4 g(dp/dc)/AF\mu D^2$ , where  $A$  is the electrode area. The point in Fig. 2A where the lines intersect is the threshold, which determines  $Ra_c$  as  $1350 \pm 300$ , in reasonable agreement with theory.

Other results of this analysis are also reasonable. The ratio of the slopes of the lines in Fig. 2A is  $2.33 \pm 0.19$ , in agreement with theoretical prediction, 2.429 (14), and with thermal convection results (15). The linear dependence of  $J$  on  $Ra$  continues up to  $Ra = 23,000$ , a second known critical point (16). At  $Ra > 100,000$  we observed persistent, small ( $\approx 1 \text{ mV}$ ), semiperiodic oscillations in  $V$  that may evidence turbulence.

The damped oscillations when the current is first turned on arise in the following way. Before convection begins, the  $\text{Fe}^{II}$  and  $\text{Fe}^{III}$  concentrations are horizontally stratified. After convection is fully developed, they are organized in Benard cells of linear dimension  $\approx d$ . It takes a finite time,  $\approx d^2/D$ , for the composition to change from one profile to the other. But meanwhile, the fluid is turned upside down once each half cycle of the convective motion, and remnants of the initial composition profiles, while they persist, are carried cyclically from one electrode to the other, making  $V(t)$  oscillate up and down. When the current is turned off, the fluid motion continues for

half an orbit more and  $V(t)$  reverses sign before it decays away.

We are surprised that effects so striking in an experiment so simple have not been reported before. The prior work most comparable to ours was that of Baranowski and Kawczynski (9), who applied current steps to horizontal copper electrodes and a  $\text{Cu}^{2+}$ -containing electrolyte. They also observed a decrease in voltage at the onset of convection but did not see oscillations or voltage reversals. Perhaps these phenomena have been seen before by others but, as with us many years ago (17), only as minor side effects ignored in the pursuit of more pressing concerns. The phenomena may have a use, however. Large-scale convection processes in the earth, the ocean, the atmosphere, and the sun can all be modeled by Rayleigh-Benard convection. Experimental simulation of them with electrochemical analogs would be easier than with thermal techniques, especially if one wishes to investigate transient effects.

WILLIAM J. WARD III

OLIVER H. LE BLANC, JR.

General Electric Research and  
Development Center,  
Schenectady, New York 12301

#### References and Notes

1. The cell was a hollow Plexiglas cylinder, 2.5 cm inside diameter, into each end of which was inserted a piston with a platinum foil electrode covering its end face. The spacing was fixed to a few percent by including a small piece of glass or Teflon of known thickness.
2. The  $\text{HCl}$  served as indifferent electrolyte and to fix  $\text{H}^+$  and  $\text{Cl}^-$  activities. Similar effects were seen with  $0.05M$   $\text{FeCl}_2$  and  $\text{FeCl}_3$  with  $0.1M$   $\text{HCl}$  or  $1M$  or  $0.1M$   $\text{KCl}$  as indifferent electrolyte or none at all and with  $0.05M$  ferrous and ferric sulfates or perchlorates and  $1N$   $\text{H}_2\text{SO}_4$  or  $\text{HClO}_4$ , respectively. We use the nomenclature

- Fe<sup>II</sup> and Fe<sup>III</sup> to indicate that Fe<sup>2+</sup> and Fe<sup>3+</sup> exist in Cl<sup>-</sup> media in complexes with Cl<sup>-</sup>. The value of  $dp/dc$  is largely determined by the mass of the counterion; it is about four times larger with ClO<sub>4</sub><sup>-</sup> than with Cl<sup>-</sup>.
3. H. S. Carslaw and J. C. Jaeger, *Conduction of Heat in Solids* (Oxford Univ. Press, London, 1959), p. 113, case ii.
  4. R. W. DeBlois suggested this.
  5. H. Benard, *Rev. Gen. Sci.* **12**, 1261, 1309 (1900); *Ann. Chim. Phys.* **23**, 62 (1901); S. Chandrasekhar, *Hydrodynamic and Hydromagnetic Stability* (Oxford Univ. Press, London, 1961); F. H. Busse, *Rep. Prog. Phys.* **41**, 1929 (1978); *Topics Appl. Phys.* **45**, 97 (1981).
  6. Lord Rayleigh, *Philos. Mag.* **32**, 529 (1916).
  7. J. S. Turner, *Buoyant Effects in Fluids* (Cambridge Univ. Press, Cambridge, 1973).
  8. E. J. Fenech and C. W. Tobias, *Electrochim. Acta* **2**, 311 (1960); M. Blair and J. A. Quinn, *J. Fluid Mech.* **36**, 385 (1969); C. W. Tobias and R. G. Hickman, *Z. Phys. Chem.* **229**, 145 (1965); F. R. McLarnon, R. H. Müller, C. W. Tobias, *J. Electrochem. Soc.* **129**, 2201 (1982).
  9. B. Baranowski and A. I. Kawczynski, *Electrochim. Acta* **17**, 695 (1972).
  10. J. S. Newman, *Electrochemical Systems* (Prentice-Hall, New York, 1973), pp. 254-265.
  11. V. G. Levich, *Physicochemical Hydrodynamics* (Prentice-Hall, Englewood Cliffs, N.J., 1962), pp. 279, 294-297.
  12. By measuring static *i-V* characteristics with the cathode up as a function of FeCl<sub>2</sub> and FeCl<sub>3</sub> concentrations in 1M HCl [A. T. Hubbard and F. C. Anson, in *Electroanalytical Chemistry*, A. J. Bard, Ed. (Dekker, New York, 1970), vol. 4, p. 129, Eq. 84].
  13. The Schmidt number is therefore  $1.4 \times 10^3$ .
  14. A. Schluter, D. Lortz, F. Busse, *J. Fluid Mech.* **23**, 129 (1965).
  15. H. T. Rossby, *ibid.* **36**, 309 (1969).
  16. W. V. R. Malkus, *Proc. R. Soc. London Ser. A* **225**, 185 (1954); F. H. Busse, *J. Math. Phys.* **46**, 140 (1967); R. Krishnamurti, *J. Fluid Mech.* **42**, 295 (1970).
  17. W. J. Ward, *Nature (London)* **227**, 162 (1970).
  18. We thank F. H. Busse, N. Ivory, F. R. McLarnon, J. W. Flock, C. S. Herrick, A. N. Liao, L. W. Niedrach, and A. W. Urquhart, who suggested ways to improve our manuscript.

16 March 1984; accepted 9 July 1984

## Human T-Cell Leukemia Virus (HTLV-I) Antibodies in Africa

**Abstract.** Antibodies specific for human T-cell leukemia-lymphoma virus type I (HTLV-I) were demonstrated in serum samples from various groups of people in South Africa, Uganda, Ghana, Nigeria, Tunisia, and Egypt. The samples had been collected for other purposes and were presumably selected without bias toward clinical conditions associated with HTLV infections. Regional differences in antibody positivity were observed, indicating widely distributed loci of occurrence of HTLV on the African continent in people of both black and white ancestry. Two patients with high titers of antibody to HTLV-I had some signs of adult T-cell leukemia-lymphoma. In several groups a high frequency of false positive serum reactions was indicated when specific confirmation steps were included in the assay. Further characterization of these sera revealed highly elevated immunoglobulin levels, possibly due to polyclonal activation of immunoglobulin synthesis in these subjects. The possibility that related cross-reactive human retroviruses coexist in the same groups was not eliminated.

The human T-cell leukemia-lymphoma viruses (HTLV) are a family of related retroviruses originally isolated in the United States from patients with T-cell lymphoma and cutaneous manifestations (1). A particular subgroup of the family, HTLV type I, is linked to the cause of these malignancies, which share clinical and epidemiologic features with the disease called adult T-cell leukemia-lymphoma (ATL) that occurs in certain regions of Japan (2, 3) and in persons of African ancestry in the Caribbean Basin (4) and in the southeastern United States (5). An atypical chronic lymphocytic leukemia in Nigeria is also suggestive of an association with HTLV (6), as is the high incidence of antibodies cross-reactive with HTLV-I in Old World primates captured in Kenya and Ethiopia and housed in West Germany (7) and the United States and Russia (8). Although the mechanism of transmission of HTLV is currently unknown, horizontal transmission is clearly implicated by molecular and epidemiologic analyses (9, 10). HTLV seropositivity in regions endemic for ATL is elevated overall in the general population and further elevated among

close family members of cases and in recipients of blood transfusions (11, 12).

The present study, which is mainly descriptive, was undertaken to investigate the occurrence of antibodies to HTLV-I in various groups of people in widely distributed areas of the African continent. We studied serum samples that had been collected for surveys of diseases with no known association with HTLV-I and samples from hospital-based clinic patients. We used a highly sensitive enzyme-linked immunosorbent assay (ELISA) to detect antibodies to HTLV-I (13) (see Table 1). Because of the diversity of the test groups, our data cannot be used to make strict epidemiological comparisons, but can be used as a means to compare the distribution of virus antibody positivity with previously reported studies of exposure to the virus (2, 12, 14) in similar or analogous groups.

The testing procedure was performed in two steps (legend to Table 1). In step 1, all samples were screened to determine quantitative levels of antibody binding to HTLV-I. In step 2, "candidate" positive sera were selected and tested for specificity in one or more

confirmatory steps. The screen-test results are expressed as a ratio (*R*) to a standard reference normal serum to control daily variations in test results (13). The threshold level,  $R \geq 2$ , was not expected to exclude negative sera. The use of this cutoff for confirmation was based on prior experience with normal U.S. blood donors where samples with a screening ratio of  $<2$  are negative in the confirmation assay. This reference normal serum level and the threshold for detection of sera confirmed as being positive for antibody to HTLV-I were derived from an analysis of 1210 U.S. blood donors (15).

Specificity was considered confirmed when sera passed either one of the confirmatory tests described in Table 1. The accuracy and precision of the antibody-blocking procedure was verified by measuring the fractional reduction of antibody binding for mixtures containing a predetermined ratio of HTLV-positive antibodies to the reference normal serum. The results plotted in Fig. 1 show excellent agreement with the predicted results at low levels of positive antibody and deviation within acceptable limits due to incomplete blockade at the higher levels of human antibody. Of those sera failing confirmation by antibody blocking, only three were confirmed by absorption with virus-positive cells.

The values for the numbers of sera from the groups exceeding the screen-test threshold and for the numbers of confirmed positive sera in each of these groups are presented in Table 1. The median values for screen ratio (*R*) within the groups were in most cases close to the median value of 1.17 found for U.S. donors (15). However, median values of *R* for samples from Tunisia and Ghana were two to three times higher. This reflected the absence of a simple correlation between the prevalence of confirmed positive sera and the proportion of sera exceeding the screen threshold level ( $R \geq 2$ ); for example, the proportion of confirmed positive donors in the Ugandan group (21 percent, which was highest of all groups) was two times higher, while the proportion of samples exceeding  $R \geq 2$  was only one-half that of the Ghanaian groups.

We investigated some of the reasons for this apparent high rate of false positivity. Among the Ghanaian samples, 28 out of 67 with high ratios ( $R \geq 6$ ) were nonconfirmed. The mean and median immunoglobulin G (IgG) levels of these 28 samples were, respectively, 130 and 106 mg/ml compared to 9 mg/ml for the standard control serum (measured by ELISA with immunopurified goat antise-